Development 135, 3379-3388 (2008) doi:10.1242/dev.024612

Rewiring the retinal ganglion cell gene regulatory network: Neurod1 promotes retinal ganglion cell fate in the absence of Math5

Chai-An Mao[1], Steven W. Wang[2], Ping Pan[1] and William H. Klein[1,3,*]

Retinal progenitor cells (RPCs) express basic helix-loop-helix (bHLH) factors in a strikingly mosaic spatiotemporal pattern, which is thought to contribute to the establishment of individual retinal cell identity. Here, we ask whether this tightly regulated pattern is essential for the orderly differentiation of the early retinal cell types and whether different bHLH genes have distinct functions that are adapted for each RPC. To address these issues, we replaced one bHLH gene with another. *Math5* is a bHLH gene that is essential for establishing retinal ganglion cell (RGC) fate. We analyzed the retinas of mice in which *Math5* was replaced with *Neurod1* or *Math3*, bHLH genes that are expressed in another RPC and are required to establish amacrine cell fate. In the absence of *Math5*, $Math5^{Neurod1\text{-}KI}$ was able to specify RGCs, activate RGC genes and restore the optic nerve, although not as effectively as *Math5*. By contrast, $Math5^{Math3\text{-}KI}$ was much less effective than $Math5^{Neurod1\text{-}KI}$ in replacing Math5. In addition, expression of *Neurod1* and *Math3* from the $Math5^{Neurod1\text{-}KI/Math3\text{-}KI}$ allele did not result in enhanced amacrine cell production. These results were unexpected because they indicated that bHLH genes, which are currently thought to have evolved highly specialized functions, are nonetheless able to adjust their functions by interpreting the local positional information that is programmed into the RPC lineages. We conclude that, although Neurod1 and Math3 have evolved specialized functions for establishing amacrine cell fate, they are nevertheless capable of alternative functions when expressed in foreign environments.

KEY WORDS: Retinal ganglion cells, Retinal progenitor cells, bHLH genes, *Math5* (*Atoh7*), *Neurod1*, *Math3* (*Neurod4*)

INTRODUCTION

In vertebrates, postmitotic retinal neurons are generated from a pool of multipotent retinal progenitor cells (RPCs) in a temporal order: retinal ganglion cells (RGCs) are produced first, followed immediately by amacrine cells, horizontal cells and cone photoreceptor cells in highly overlapping waves of cell differentiation. Subsequent to the formation of these early neuronal cell types, the later cell types form: bipolar cells, rod photoreceptor cells and, lastly, Müller glial cells. Distinct RPCs integrate their intrinsic programs with local environmental signals to define their competence states and to commit to individual retinal cell fates (Livesey and Cepko, 2001). Many transcription factors have been implicated in setting up the competence states of RPCs (Hatakeyama and Kageyama, 2004; Ohsawa and Kageyama, 2008). In the mouse, *Math5* (*Atoh7* – Mouse Genome Informatics), an ortholog of the *Drosophila* bHLH proneural gene *Atonal*, is expressed in a subpopulation of RPCs and is essential for establishing RGC competence (Brown et al., 1998; Brown et al., 2001; Wang et al., 2001; Yang et al., 2003; Mu et al., 2005).

A remarkable feature of retinal development is that RPCs are capable of simultaneously producing multiple cell types, suggesting the presence of subpopulations RPCs with each possessing a distinct genetic makeup. Unfortunately, these genetically distinct RPC subpopulations have not been clearly defined by conventional cell lineage tracing experiments (reviewed by Mu and Klein, 2004; Mu and Klein, 2008). The bHLH genes *Math5*, *Mash1* (*Ascl1* – Mouse Genome Informatics), *Math3* (*Neurod4* – Mouse Genome Informatics) and *Neurod1* are expressed in the developing retina at overlapping times but in largely distinct, interspersed RPC subpopulations (Vetter and Brown, 2001; Akagi et al., 2004; Hatakeyama and Kageyama, 2004; Le et al., 2006; Ohsawa and Kageyama, 2008; Trimarchi et al., 2008). The bHLH factors collaborate with homeobox factors to specify particular retinal cell fates at the expense of others (Wang and Harris, 2005; Cayouette et al., 2006; Ohsawa and Kageyama, 2008). However, in early developing retina, many key homeobox genes, such as *Pax6* and *Six3*, are expressed in virtually all RPCs (Lagutin et al., 2001; Bäumer et al., 2003) and have multiple functions in specifying distinct cell fates (Ohsawa and Kageyama, 2008). It is therefore likely that the mosaic expression pattern of bHLH genes more accurately mirrors the state of competency within each individual RPC for the early retinal cell types (Cayouette et al., 2006). This concept implies that a unique bHLH gene expression pattern regulates the competence state of each RPC fate for the early differentiating cell types, with more widely expressed homeobox factors acting in conjunction with the bHLH factors. Thus, replacing one bHLH gene with another might be expected to redirect the RPC to assume the competence state defined by the replacing bHLH gene. However, it is also possible that this type of replacement would not be tolerated because the replacing bHLH gene, which might have evolved specialized functions in the retina, would be incapable of integrating into the intrinsic program of a foreign RPC. A final possibility is that replacing one bHLH gene with another would restore the original RPC lineage. If this were the case, it would suggest that retinal bHLH genes might not be highly specialized and therefore are susceptible to the intracellular environment of the foreign RPC.

[1]Department of Biochemistry and Molecular Biology, The University of Texas M. D. Anderson Cancer Center, Houston, TX 77030, USA. [2]Department of Ophthalmology and Visual Science, The University of Texas Houston Medical School, Houston, TX 77030, USA. [3]Training Program in Genes and Development, The University of Texas Graduate School of Biomedical Sciences at Houston, Houston, TX 77030, USA.

*Author for correspondence (e-mail: whklein@mdanderson.org)

Accepted 26 August 2008

To determine which of these possibilities actually occurs, we replaced *Math5* with either *Neurod1* or *Math3*, which are required together for establishing amacrine cell fate, and are capable of producing excess numbers of amacrine cells when each of them is ectopically co-expressed with Pax6 or Six3 (Inoue et al., 2002). Here, we demonstrate that Neurod1 can partially rescue the functions of Math5 in RGC production. By contrast, Math3 could only modestly rescue Math5 mutant defects by activating some RGC genes. In addition, *Neurod1* and *Math3* co-expression at the *Math5* locus does not lead to the overproduction of amacrine cells. Our results demonstrate that although *Neurod1* and *Math3* have evolved specialized functions, they are nevertheless capable of alternative functions when expressed in a foreign environment. These results suggest that RPC heterogeneity is largely programmed by intrinsic mechanisms that are not solely dependent on a specific bHLH gene.

MATERIALS AND METHODS

Gene targeting and animal breeding

To construct the targeting vector, genomic DNA from G4 ES cells (George et al., 2007) was used for the polymerase chain reaction (PCR) amplification of 5 kb fragments representing the left and right homologous replacement arms from the *Math5* locus (Fig. 1B). Complete coding regions for *Neurod1* and *Math3* are located in single exons, and their sequences were amplified using G4 ES cell genomic DNA. These fragments were sequentially subcloned into a targeting vector (Mao et al., 2008). The resulting constructs were linearized and electroporated into G4 ES cells, after which G418-resistent ES cells were selected to identify homologous recombination events. A 5′ probe from outside the homologous recombination region was used to detect 20.5 kb wild-type and 15.6 kb knock-in fragments produced by *Bam*HI digestion of ES cell DNA (Fig. 1B,C). Two targeted ES cell lines for each construct were expanded and injected into B6(GC)-$Tyr^{c\text{-}2J}$/J blastocysts, and the injected blastocysts were transferred into the uteri of pseudopregnant C57/BL/6J female mice. Chimeric males resulting from the injected blastocysts were bred to B6(GC)-$Tyr^{c\text{-}2J}$/J females (Jackson Laboratory) to generate $Math5^{Neurod1\text{-}KI/+}$ and $Math5^{Math3\text{-}KI/+}$ heterozygotes. The two lines were subsequently bred to $Math5^{lacZ\text{-}KI/+}$ mice (Wang et al., 2001) to generate $Math5^{Neurod1\text{-}KI/lacZ\text{-}KI}$ and $Math5^{Math3\text{-}KI/lacZ\text{-}KI}$ lines. $Math5^{Neurod1\text{-}KI}$, $Math5^{Math3\text{-}KI}$, $Math5^{lacZ\text{-}KI}$ and *Math5* wild-type alleles were distinguished using a Southern blot genome hybridization probe and *Eco*RV-digested genomic DNA (see Fig. 1D). Embryos were designated as embryonic day 0.5 (E0.5) at noon on the day in which vaginal plugs were observed.

All animal procedures in this study followed the US Public Health Service Policy on Humane Care and Use of Laboratory Animals and were approved by the Institutional Animal Care and Use Committee at The University of Texas M. D. Anderson Cancer Center.

Histology, in situ hybridization and immunohistochemical analysis

Embryos and eyes dissected from embryos or adults were fixed, paraffin-embedded and sectioned into 7 μm or 12 μm slices for immunohistochemical analysis or in situ hybridization, respectively, as described by Mao et al. (Mao et al., 2008). After de-waxing and rehydration, the sections were stained with Hematoxylin and Eosin before further analysis. In situ hybridization was performed as described by Mu et al. (Mu et al., 2004).

For immunohistochemical analysis, sections were placed in a microwave oven at 600 W in 10 mM sodium citrate for 15 minutes to expose the antigen epitopes. Microwave-treated sections were then incubated with the primary antibodies listed below. For indirect immunofluorescence, a tyromide signal amplification kit (TSA biotin system, PerkinElmer) was used for Neurod1 and Eomes to optimize signal intensity. For double immunofluorescence, Alexa-conjugated secondary antibodies (Invitrogen) were used. The primary antibodies were anti-Brn3b/Pou4f2 (Santa Cruz Biotech, 1:200 dilution), anti-Chx10 (Exalpha, 1:1000 dilution), anti-GSK3β (Cell Signaling, 1:400 dilution), anti-NFL (Invitrogen, 1:250 dilution), anti-NF160 (DSHB, 1:1000 dilution), anti-Isl1 (DSHB, 1:250 dilution), anti-melanopsin (provided by Satchidananda Panda, Salk Institute), anti-SMI32 (Covance, 1:1000 dilution), anti-Tbr2/Eomes (Chemicon, 1:1000 dilution), anti-Sox9 (Chemicon, 1:200 dilution), anti-TUJ1 (Covance, 1:500 dilution), anti-ChAT (Chemicon, 1:100 dilution), anti-opsin(R/G) (Chemicon, 1/200 dilution), anti-calrectinin (Chemicon, 1:2500 dilution), anti-calbindin (Swant, 1:5000 dilution), anti-Pax6 (DSHB, 1:200 dilution) and anti-p57 (Santa Cruz, 1:40 dilution). Horseradish peroxidase-conjugated secondary antibody for tyromide signal amplification was obtained from Jackson ImmunoResearch. To detect RGC axons, anti-NFL antibody was used to stain flat-mounted adult retinas (Mao et al., 2008). The number of axonal bundles and the axonal density within each bundle were analyzed with the same settings using SimplePCI software (Compix, Sewickley, PA) to automatically select regions of interest from the peripheral retinal flat-mount images. Flat-mount immunostaining was also used to monitor the distribution of melanopsin and SMI-32 positive RGCs. For quantifying RGC specification during embryonic stages, Pou4f2-positive cells were used to estimate RGC number. Three retinal sections (three sections apart) collected from littermates of different genotypes were stained with anti-Brn3b/Pou4f2 antibody, and the number of Pou4f2-positive cells on each section was counted on an Olympus Fluoview 1000 confocal microscope.

Quantitative reverse transcriptase-PCR analysis

Total RNA were collected from two E13.5 retinas using TRIZOL reagent (Invitrogen, CA). RNAs were reversed transcribed using Superscript First-Strand Synthesis System for reverse transcriptase (RT)-PCR (Invitrogen) following the manufacturer's instruction. One twentieth of the total cDNAs was amplified for quantitative (q)PCR using SYBR green PCR master mix (Applied Biosystems, CA). The relative expression levels were normalized to that of GAPDH and calculated using the comparative C_t method (7500 Fast Real-time PCR systems SDS software, Applied Biosystems). DNA sequences of PCR primers indicated were: Math5 5′UTR forward, 5′-TCCGTCTGTGTCTTATTCACTC-3′; Math5 reverse, 5′-TTTGCAGGCCGACTTCATCCTC-3′; Math3 reverse, 5′-ATATACATTTTTGCCATGGCCGC-3′; GAPDH forward, 5′-AGGTCGGTGTGAACGGATTTG-3′; GAPDH reverse, 5′-TGTAGACCATGTAGTTGAGGTCA-3′.

RESULTS

Expression of *Neurod1* and *Math3* in $Math5^{Neurod1\text{-}KI}$ and $Math5^{Math3\text{-}KI}$ embryonic retinas

The bHLH sequences from *Math5*, *Neurod1* and *Math3* are similar but not identical, clustering together with the other mouse bHLH genes (Fig. 1A) (Ledent et al., 2002). Outside of the bHLH domain, significant differences in *Math5*, *Neurod1* and *Math3* sequences indicate that these bHLH genes have undergone extensive divergence since their emergence from a common ancestral gene. A sequence tree shows that *Math5* is rooted in a clade distinct from that of *Neurod1* and *Math3*, and that *Neurod1* and *Math3* are closely related to each other in their bHLH domains (Fig. 1A). To determine the effects of replacing *Math5* with *Neurod1* or *Math3*, we used targeting constructs to target embryonic stem (ES) cells in which we removed the entire *Math5* sequence and replaced it with either a *Neurod1* or a *Math3* sequence (Fig. 1B). Germline mice containing $Math5^{Neurod1\text{-}KI}$ or $Math5^{Math3\text{-}KI}$ alleles were bred to $Math5^{lacZ\text{-}KI/lacZ\text{-}KI}$ mice (*Math5*-null mice) and to each other to generate mice with the following genotypes: $Math5^{Neurod1\text{-}KI/+}$ (Fig. 1C), $Math5^{Neurod1\text{-}KI/lacZ\text{-}KI}$, $Math5^{Neurod1\text{-}KI/Neurod1\text{-}KI}$ (Fig. 1D), $Math5^{Math3\text{-}KI/+}$, $Math5^{Math3\text{-}KI/lacZ\text{-}KI}$, $Math5^{Math3\text{-}KI/Math3\text{-}KI}$ and $Math5^{Neurod1\text{-}KI/Math3\text{-}KI}$.

We first determined whether $Math5^{Neurod1\text{-}KI}$ and $Math5^{Math3\text{-}KI}$ alleles were expressed in a pattern mimicking that of *Math5*. At E12.5, we detected low expression levels of Neurod1 protein in the retinas of wild-type mice (Fig. 1E). By contrast, high levels of Neurod1 expression were observed in $Math5^{Neurod1\text{-}KI/Math3\text{-}KI}$

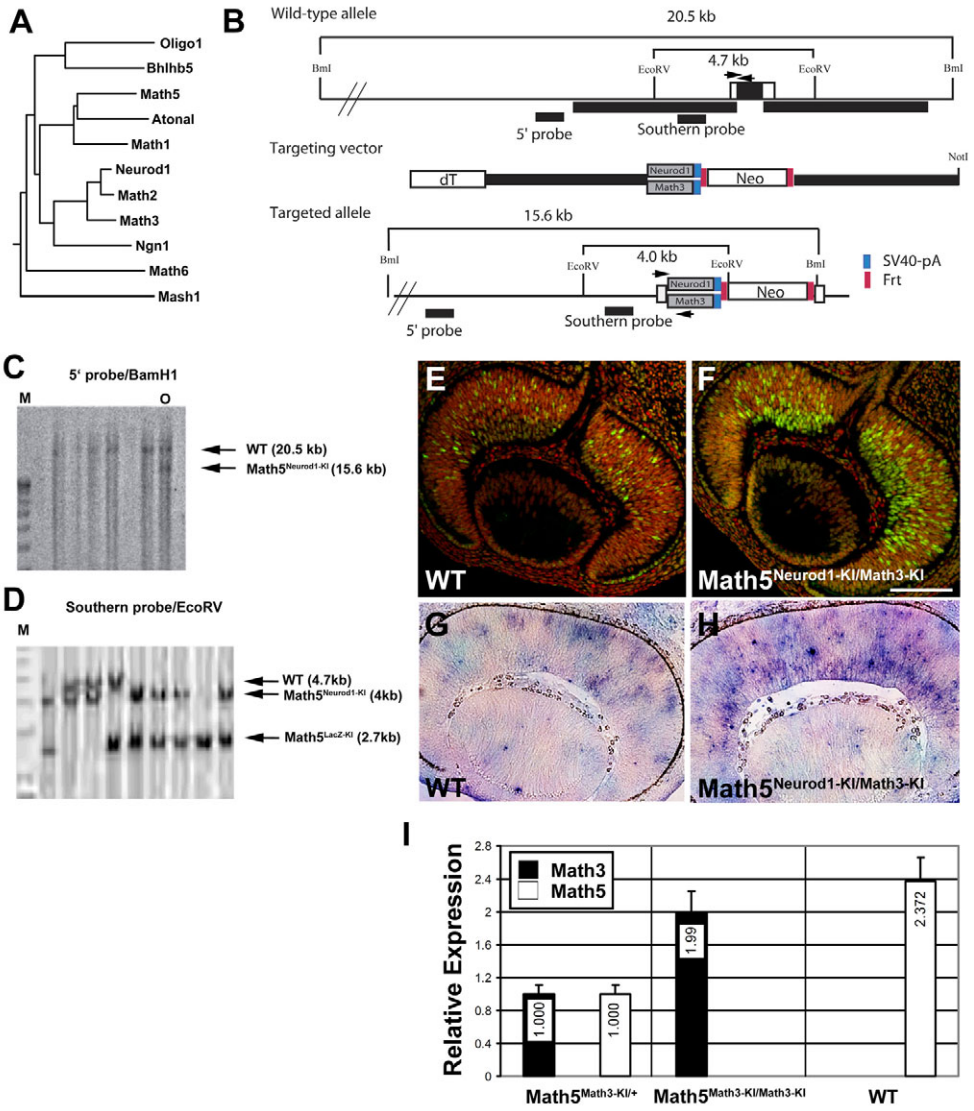

Fig. 1. Replacing endogenous *Math5* with *Neurod1* or *Math3*. (**A**) Sequence relationships among bHLH domains of representative proneural bHLH genes [method described by Ledent et al. (Ledent et al., 2002)]. Mash1 was chosen as the outgroup. Branch lengths are proportional to the distance between the sequences. (**B**) Genome structure for *Math5*, the targeting construct and the predicted structure of the targeted *Neurod1* and *Math3* knock-in alleles. The single *Math5* exon is depicted as a black box. The black bars underneath indicate the DNA fragments amplified from genomic DNA for the targeting construct. Red boxes depict FRT recombination sites. Blue boxes indicate SV40-pA sequence. Black arrows indicated the PCR primers used to amplify Math5 and Math5$^{Math3\text{-}KI}$ for qRT-PCR analysis. The primer sequences are described in the Materials and methods. (**C**) Representative Southern blot analysis using the 5′ probe to distinguish *Math5* wild-type and *Math5*$^{Neurod1\text{-}KI}$ alleles from genomic DNA of targeted ES cells. O indicates a targeted ES cell. (**D**) Representative Southern blot analysis using the Southern probe depicted in B to distinguish *Math5* wild-type, *Math5*$^{Neurod1\text{-}KI}$ and *Math5*$^{lacZ\text{-}KI}$ alleles from tail genomic DNA of littermates resulting from a *Math5*$^{Neurod1\text{-}KI/lacZ\text{-}KI}$ × *Math5*$^{lacZ\text{-}KI/+}$ cross. (**E-H**) Misexpression of *Neurod1* and *Math3* from the *Math5* locus. Retinal sections from E12.5 wild-type (E,G) and *Math5*$^{Neurod1\text{-}KI/Math3\text{-}KI}$ (F,H) embryos were immunostained with anti-Neurod1 antibody (E,F) or labeled with a *Math3* antisense probe by in situ hybridization (G,H). The images in G and H have been enhanced using Photoshop. (**I**) qRT-PCR analysis of *Math5* and *Math5*$^{Math3\text{-}KI}$ alleles. Gene expression levels were normalized to the expression of endogenous GAPDH transcripts. Scale bar: 100 μm.

retinas at E12.5 (Fig. 1F). Similar to *Neurod1* protein expression, *Math3* transcript expression, although weak, was readily detectable near the ventricular region in E12.5 wild-type retinas, and in a pattern similar to that of Neurod1 expression in *Math5*$^{Neurod1\text{-}KI/Math3\text{-}KI}$ retinas at the same developmental time (Fig. 1G,H). Between E12.5 and E15.5, the expression of *Neurod1* and *Math3* from the *Math5*$^{Neurod1\text{-}KI}$ and *Math5*$^{Math3\text{-}KI}$ alleles closely resembled endogenous *Math5* expression, indicating that ectopic *Neurod1* and *Math3* expression was under the control of the Math5 regulatory region. Furthermore, *Neurod1* expression did not differ between retinas with *Math5*$^{Neurod1\text{-}KI/+}$ or *Math5*$^{Neurod1\text{-}KI/Neurod1\text{-}KI}$ genotypes, indicating the accurate replacement of *Math5* by *Neurod1* (data not shown). To determine whether the knock-in *Math3* allele expressed transcripts at the same level as the wild-type *Math5* allele, we compared the expression levels of *Math5* and *Math5*$^{Math3\text{-}KI}$ alleles at E13.5. Fig. 1I shows that *Math5* and *Math5*$^{Math3\text{-}KI}$ alleles were expressed at similar levels in *Math5*$^{Math3\text{-}KI/+}$ retinas, and that *Math5*$^{Math3\text{-}KI}$ in *Math5*$^{Math3\text{-}KI/Math3\text{-}KI}$ retinas was expressed at levels corresponding to those of *Math5* in wild-type retinas.

Partial restoration of RGC axons, optic nerves, and RGC subtypes with *Math5*$^{Neurod1\text{-}KI}$ and *Math5*$^{Math3\text{-}KI}$ alleles

Math5-null mice have severe optic nerve hypoplasia and in extreme cases lack optic nerves entirely (Fig. 2A) (Brown et al., 2001; Wang et al., 2001). Eyes from adult *Math5*$^{Neurod1\text{-}KI/lacZ\text{-}KI}$ and *Math5*$^{Neurod1\text{-}KI/Math3\text{-}KI}$ mice 4-5 weeks old (P30) were often found attached to well-developed optic nerves with diameters that were 50-60% those of wild-type mice (Fig. 2A,B). Histological sections from *Math5*$^{Neurod1\text{-}KI/lacZ\text{-}KI}$ and *Math5*$^{Neurod1\text{-}KI/Math3\text{-}KI}$ mice also revealed substantial restoration of optic nerves (Fig. 2A1,A2,B). Immunostaining retinas with a Pou4f2/Brn3b antibody, which detects RGCs, showed that 30-40% of the cells in the ganglion cell layer

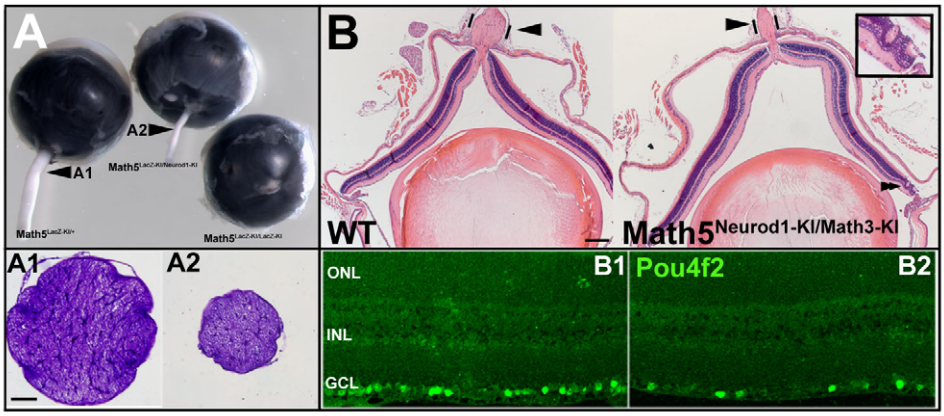

Fig. 2. Neurod1 and Math3 partially restore the optic nerve in *Math5*-null mice. (**A**) Dissected eyes from P30 mice. From left to right: *Math5*$^{lacZ\text{-}KI/+}$, *Math5*$^{Neurod1\text{-}KI/lacZ\text{-}KI}$ and *Math5*$^{lacZ\text{-}KI/lacZ\text{-}KI}$. (**A1**,**A2**) Cross-sections of the optic nerves from *Math5*$^{lacZ\text{-}KI/+}$ and *Math5*$^{Neurod1\text{-}KI/lacZ\text{-}KI}$ dissected eyes shown in A were stained with Cresyl Fast Violet. (**B**) Histological sections of P30 eyes from wild-type and *Math5*$^{Neurod1\text{-}KI/Math3\text{-}KI}$ littermates. Arrowheads indicate the optic nerves. The double arrowhead indicates a rosette structure sometimes seen in *Math5*$^{Neurod1\text{-}KI/Math3\text{-}KI}$ retinas (inset). (**B1**,**B2**) Pou4f2 expression in wild-type and *Math5*$^{Neurod1\text{-}KI/Math3\text{-}KI}$ retinal sections. Representative lateral regions were used for comparison. ONL, outer nuclear layer; INL, inner nuclear layer; GCL, ganglion cell layer. Scale bars: 50 μm in A1; 200 μm in B.

(GCL) of *Math5*$^{Neurod1\text{-}KI/Math3\text{-}KI}$ retinas expressed Pou4f2 compared with wild-type retinas (Fig. 2B1,B2). By contrast, we never observed optic nerves in the eyes of *Math5*$^{Math3\text{-}KI/lacZ\text{-}KI}$ mice, despite the close relationship between the *Neurod1* and *Math3* genes. These results indicated that *Neurod1*, but not *Math3*, was capable of partially restoring optic nerves in *Math5*-deficient mice.

The presence of optic nerves in *Math5*$^{Neurod1\text{-}KI/Math3\text{-}KI}$ and *Math5*$^{Neurod1\text{-}KI/lacZ\text{-}KI}$ mice suggested that RGC axons were forming and extending into the optic disk. Immunostaining of flat-mount retinas from P30-P40 mice with an anti-neurofilament light chain (NFL) antibody revealed that one-third (4/12) of *Math5*$^{Neurod1\text{-}KI/Math3\text{-}KI}$ and two-thirds (4/6) of *Math5*$^{Neurod1\text{-}KI/lacZ\text{-}KI}$ retinas had significantly greater numbers and higher density of RGC axon bundles compared with *Math5*-null retinas (Fig. 3A-D). Although some axons appeared misoriented, the majority of axons were well bundled and oriented towards the optic disk (Fig. 3C,D).

The lack of a complete rescue of the optic nerve in the knock-in retinas might be explained by enhanced apoptosis; a significant increase in cell death was detected in *Math5*$^{Neurod1\text{-}KI/lacZ\text{-}KI}$ and *Math5*$^{Neurod1\text{-}KI/Math3\text{-}KI}$ retinas from E11.5 to E16.5 compared with wild-type controls (data not shown). No differences in RGC axon number or density were detected when *Math5*$^{Neurod1\text{-}KI/+}$ and *Math5*$^{Math3\text{-}KI/+}$ retinas were compared with wild-type controls (data not shown). The results demonstrated that Neurod1 could partially replace Math5 in restoring RGC axons and that Math3 alone could not replace Math5.

In the mouse retina, RGCs have been categorized into ~12-14 subtypes by morphological criteria (Sun et al., 2002; Coombs et al., 2006). Across the GCL, RGC subtypes display regular spacing between cell bodies, and arborize within precise strata of the inner plexiform layer (IPL). To determine whether RGC subtypes formed in *Math5*$^{Neurod1\text{-}KI/Math3\text{-}KI}$ retinas, we selected two previously characterized RGC subtype markers, melanopsin and SMI-32 (Lin et al., 2004), and performed immunostaining with flat-mount retinas. Melanopsin-expressing RGCs have small somata (~20 μm) and their dendrites run through the IPL, terminating at layer 1 immediately underneath the inner nuclear layer (INL). SMI-32 is expressed in RGCs with large somata (~30 μm). Melanopsin- and SMI-32-expressing RGCs both displayed a nonrandom mosaic pattern across wild-type and *Math5*$^{Neurod1\text{-}KI/Math3\text{-}KI}$ retinas (Fig. 3E-H). Additionally, the dendrites of melanopsin-expressing RGCs always arborize to layer 1 of the IPL (insets in Fig. 3E,F; n>40). These data suggest that Neurod1 can replace Math5 to specify different RGC subtypes evenly across retina, and these RGC subtypes differentiate normally with proper dendritic arborization.

Expression of RGC genes in embryonic retinas of *Math5*$^{Neurod1\text{-}KI}$ and *Math5*$^{Math3\text{-}KI}$ mice

The earliest sign of RGC differentiation begins at E12.5, when the expression of *Pou4f2* and *Isl1* is first apparent (Gan et al., 1999; Elshatory et al., 2007; Mu et al., 2008). These genes encode POU domain and LIM domain transcription factors, respectively, and both are required for RGC differentiation (Gan et al., 1999; Mu et al., 2008; Pan et al., 2008). We used anti-Pou4f2/Brn3b and anti-Isl1 antibodies to determine the expression pattern of these proteins in E13.5 retinas. In *Math5*$^{lacZ\text{-}KI/+}$ (wild-type) retinas, Pou4f2 and Isl1 were co-expressed in differentiating RGCs, as we and others have shown previously (Fig. 4A,A1,A2) (Rachel et al., 2002; Mu et al., 2008). Expression was largely absent in *Math5*$^{lacZ\text{-}KI/lacZ\text{-}KI}$ retinas (Fig. 4B,B1,B2). We found that retinas expressing *Math5*$^{Neurod1\text{-}KI}$ allele in the absence of *Math5* significantly restored the expression of Pou4f2 and Isl1 (Fig. 4C-C2,D-D2), whereas in *Math5*$^{Math3\text{-}KI/lacZ\text{-}KI}$ retinas, the expression of these early RGC markers, although detectable, was appreciably lower (Table 1). We had shown previously that expression of the neurofilament protein NF160 is strongly dependent on the presence of Pou4f2 (Mu et al., 2004). Retinas expressing the *Math5*$^{Neurod1\text{-}KI}$ allele in the absence of *Math5* had significantly higher expression of NF160 (Fig. 4A3-D3). The expression of Pou4f2, Isl1 and NF160 is indicative of RGC differentiation, and, therefore, of the number of RGCs present in the retinas of the *Math5*$^{Neurod1\text{-}KI}$ and *Math5*$^{Math3\text{-}KI}$ mice. According to this criterion, we estimated that the numbers of RGCs present in the *Math5*$^{Neurod1\text{-}KI/LacZ\text{-}KI}$ and *Math5*$^{Math3\text{-}KI/LacZ\text{-}KI}$ retinas were ~40% (173/434) and 10% (40/413), respectively, the number of RGCs in wild-type retinas (Table 1). Furthermore, the expression of Pou4f2 in *Math5*$^{Neurod1\text{-}KI/lacZ\text{-}KI}$ and *Math5*$^{Math3\text{-}KI/lacZ\text{-}KI}$ retinas was significantly lower than that in wild-type controls at E12.5,

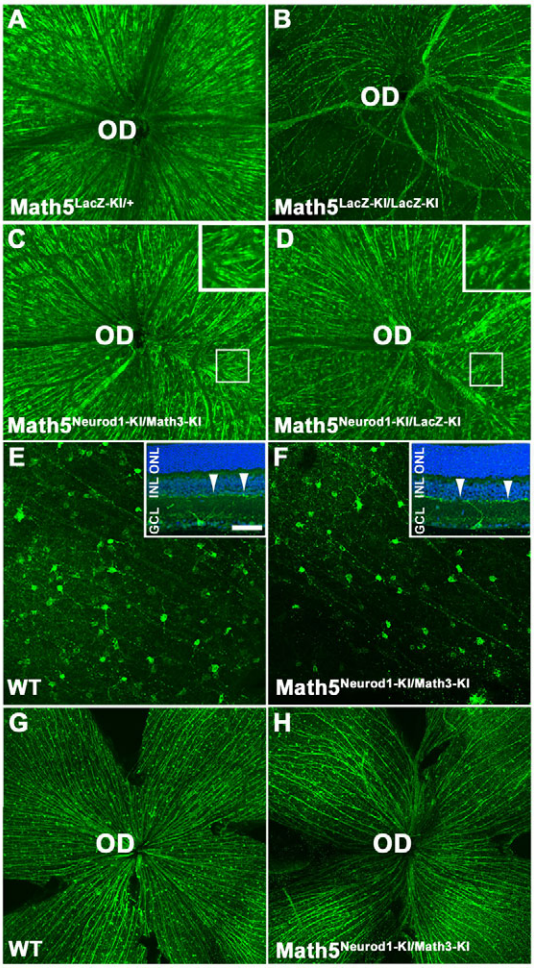

Fig. 3. Neurod1 partially restores RGC axons and RGC subtypes in the absence of Math5. (**A-D**) Immunostaining of flat-mounted retinas from P30 mice with anti-NFL antibody to reveal RGC axons. Genotypes are indicated on the lower left of each panel. Insets in C and D highlight the misoriented axons. OD, optic disk. (**E**,**F**) Representative images of immunostaining of flat-mount retinas from P30 mice using anti-melanopsin antibody to reveal the mosaic distribution pattern of melanopsin-positive RGCs. The insets in E and F show representative dendritic arborization of melanopsin-positive RGCs in layer 1 of the IPL (arrowheads). Nuclei of the three nuclear layers are stained with DAPI (blue). Scale bar: 50 μm. (**G**,**H**) Immunostaining of flat-mount retinas with anti-SMI32 antibody to show the mosaic distribution of the SMI32-positive RGC subtype.

but recovered to higher levels at E14.5 (Table 1), suggesting a delayed RGC differentiation in the *Math5*$^{Neurod1\text{-}KI/LacZ\text{-}KI}$ and *Math5*$^{Math3\text{-}KI/LacZ\text{-}KI}$ retinas.

We recently identified the T-box-containing transcription factor, eomesodermin (Eomes), as an essential factor for RGC differentiation and optic nerve formation (Mao et al., 2008). *Eomes* is a direct target gene of Pou4f2, and its expression would therefore be indicative of a functional Pou4f2 protein. At E14.5, Eomes protein is co-expressed with Pou4f2 in the innermost RGCs in wild-type retinas (Fig. 5A1-A3) (Mao et al., 2008). At this same time, Eomes is also weakly expressed in non-RGCs in the RPC proliferation layer; expression of Eomes in the innermost layer is absent in *Math5*- and *Pou4f2*-null retinas (Mao et al., 2008). Substantially more Eomes-expressing cells were observed in *Math5*$^{Neurod1\text{-}KI/Math3\text{-}KI}$ E14.5 retinas than in *Math5*-null retinas (Fig. 5B1). Similarly, more Eomes-expressing cells could be found in *Math5*$^{Neurod1\text{-}KI/lacZ\text{-}KI}$ retinas than in *Math5*-null retinas (Fig. 5C1). However, we did not detect Eomes-expressing cells in *Math5*$^{Math3\text{-}KI/lacZ\text{-}KI}$ retina (Fig. 5D1). These results suggest that Neurod1 alone can rescue Eomes expression in RGCs, but Math3 lacks this activity. By contrast, both Neurod1 and Math3 contribute to the restoration of Pou4f2 expression observed in the absence of Math5, and that Neurod1 has stronger restoration capabilities than Math3 (Fig. 5A2,B2,C2,D2; Table 1).

At E13.5 and E14.5, the numbers of Pou4f2-positive cells in the *Math5*$^{Neurod1\text{-}KI/lacZ\text{-}KI}$ (n>20) or the *Math5*$^{Math3\text{-}KI/lacZ\text{-}KI}$ (n>20) retinas were always much greater than in the *Math5*$^{lacZ\text{-}KI/lacZ\text{-}KI}$ retinas. However, we noticed that many Pou4f2-expressing cells in these knock-in retinas were abnormally positioned when compared with wild-type controls, residing in the upper-most region of the RPC layer (compare Fig. 5A2 with Fig. 5C2,D2). This suggested that RGCs expressing *Neurod1* or *Math3* in the absence of *Math5* were unable to properly migrate to the GCL. However, in *Math5*$^{Neurod1\text{-}KI/Math3\text{-}KI}$ retinas, this abnormality was partially corrected (Fig. 5B2). This result suggested that, together, Neurod1 and Math3 were slightly more effective in replacing the functions of Math5 than was Neurod1 alone.

The RGC gene regulatory network is restored in *Math5*$^{Neurod1\text{-}KI/Math3\text{-}KI}$ retinas

The partial restoration of RGC axons and optic nerves in adult retinas and the expression of the early RGC markers Pou4f2, Isl1, NF160 and Eomes in *Math5*$^{Neurod1\text{-}KI/Math3\text{-}KI}$ retinas indicated that, together, Neurod1 and Math3 could replace Math5 to activate the entire RGC gene regulatory network (Mu et al., 2004; Mu et al., 2005; Mu et al., 2008; Mu and Klein, 2008). We therefore determined the expression levels of a number of RGC-expressed genes in wild-type and *Math5*$^{Neurod1\text{-}KI/Math3\text{-}KI}$ E14.5 retinas that had various roles in RGC integrity and physiology, transcriptional regulation and extracellular signal transduction. The selected genes included those whose expression was dependent on the presence of Math5 and Pou4f2 (*Persyn*, *Gap43* and *Shh*) (Mu et al., 2004), those whose expression was dependent on Math5 but not Pou4f2 (*Myt1*, *Stmn2* and *TuJ1*) (Brown et al., 2001; Mu et al., 2005), and two genes whose dependence on Math5 and Pou4f2 has not been determined [*GDF11* (Kim et al., 2005), *Gsk3β* (Tokuoka et al., 2002) (see Table S1 in the supplementary material for details)].

Fig. 6 shows that all of the genes were expressed in RGCs of *Math5*$^{Neurod1\text{-}KI/Math3\text{-}KI}$ retinas in a similar pattern but at lower levels than in wild-type controls (compare A1-H1 with A2-H2). These results strongly suggest that the RGC gene regulatory network was activated in its entirety in *Math5*$^{Neurod1\text{-}KI/Math3\text{-}KI}$ retinas.

Because Neurod1 and Math3 are required together for amacrine cell development (Inoue et al., 2002), we determined whether increased numbers of amacrine cells were present in *Math5*$^{Neurod1\text{-}KI/Math3\text{-}KI}$ retinas. Staining with antibodies against markers for amacrine cells, including ChAT, p57Kip2, calrectinin and calbindin, revealed no differences in the numbers of cells between wild-type and *Math5*$^{Neurod1\text{-}KI/Math3\text{-}KI}$ retinas (see Fig. S1 in the supplementary material). However, we detected 20% more opsin-positive photoreceptors in *Math5*$^{Neurod1\text{-}KI/Math3\text{-}KI}$ retinas than in wild-type retinas (see Fig. S1 in the supplementary material). The significance of this modest increase was unclear,

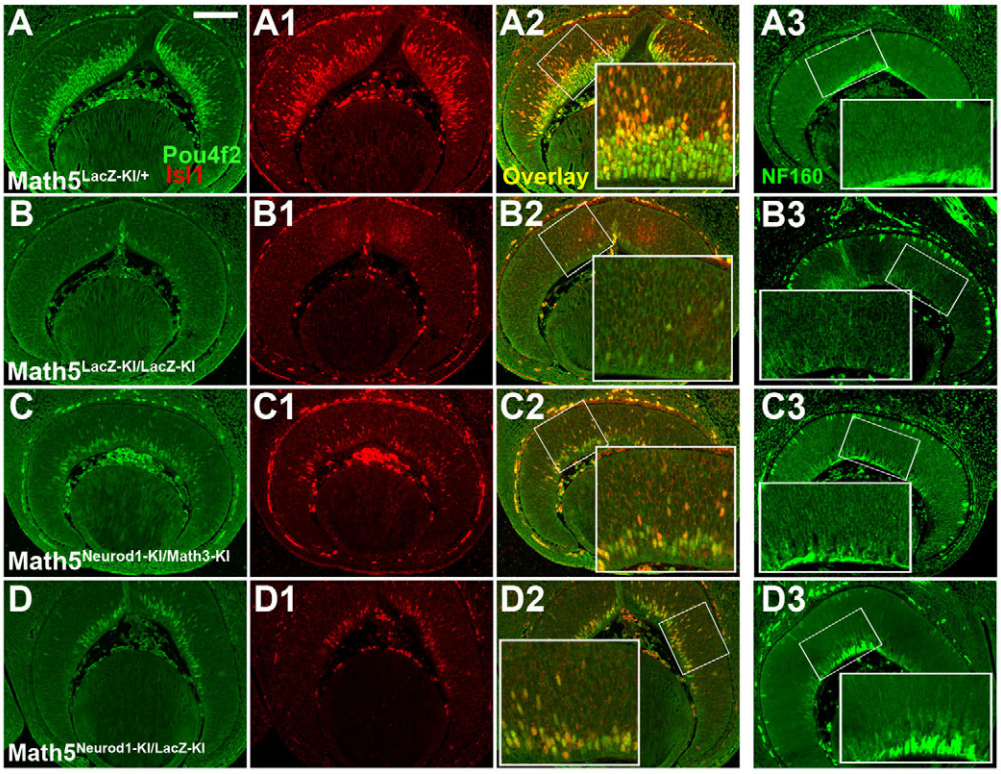

Fig. 4. Neurod1 activates early markers of RGC differentiation in the absence of Math5. (**A-D3**) Immunostaining of retinas from E13.5 embryos with anti-Pou4f2/Brn3b (A-D), anti-Isl1 (A1-D1), merged Pou4f2-Isl1 images (A2-D2) and anti-NF160 (A3-D3). Insets show higher magnification of indicated areas. (A-A3) *Math5*$^{lacZ\text{-}KI/+}$, (B-B3) *Math5*$^{lacZ\text{-}KI/lacZ\text{-}KI}$, (C-C3) *Math5*$^{Neurod1\text{-}KI/Math3\text{-}KI}$ and (D-D3) *Math5*$^{Neurod1\text{-}KI/lacZ\text{-}KI}$. Scale bar: 100 μm.

but it might reflect a re-direction of *Math5*$^{Neurod1\text{-}KI/Math3\text{-}KI}$-expressing RPCs to a photoreceptor cell fate. This might occur as a result of restored *Ngn2* expression in *Math5*$^{Neurod1\text{-}KI/Math3\text{-}KI}$ RPCs, as happens in *Math5*-null RPCs (Brown et al., 2001; Le et al., 2006). Math3, together with Mash1, is essential for bipolar cell formation (Tomita et al., 2000). We therefore determined whether increased numbers of bipolar cells could be detected in *Math5*$^{Neurod1\text{-}KI/Math3\text{-}KI}$ retinas. Fig. S1 shows that there is no difference in Chx10-positive cells in wild-type and *Math5*$^{Neurod1\text{-}KI/Math3\text{-}KI}$ retinas. The number of Sox9-positive Müller glial cells also did not change. *Math5*$^{Math3\text{-}KI/LacZ\text{-}KI}$ retina displayed histological phenotypes reminiscent of Math5-null retina, in which the numbers of all cell types normally found in the INL are reduced owing to the reduced thickness of the INL, but the ratio of each cell type was not significantly different from wild-type controls (Moshiri et al., 2008). We found that the proportion of amacrine, bipolar, horizontal and Müller cell types in the INL of *Math5*$^{Math3\text{-}KI/LacZ\text{-}KI}$ retina was similar to that of *Math5*$^{LacZ\text{-}KI/+}$ retinas (see Table S2 in the supplementary material). These data suggest that *Math3* alone does not significantly influence cell fate determination when expressed at the *Math5* locus.

Table 1. Determination of RGC numbers using anti-Pou4f2/Brn3b antibody with retinal sections from different genotypes and developmental stage

Math5$^{Neurod1\text{-}KI/+}$ × *Math5*$^{Math3\text{-}KI/+}$	E12.5	E13.5	E14.5
Wild type	181.3±3.8	292.7±12.2	829±18.7
Math5$^{Neurod1\text{-}KI/Math3\text{-}KI}$	19.3±1.8	109±6.7	532.7±14.2
Math5$^{Neurod1\text{-}KI/LacZ\text{-}KI}$ × *Math5*$^{LacZ\text{-}KI/+}$	E12.5	E13.5	E14.5
Math5$^{LacZ\text{-}KI/+}$	189.7±3.6	433.7±14.4	601±14.7
Math5$^{LacZ\text{-}KI/LacZ\text{-}KI}$	2.3±0.4	8.7±0.4	NA
Math5$^{Neurod1\text{-}KI/LacZ\text{-}KI}$	29.3±3.8	173±5.33	413.7±14.9
Math5$^{Math3\text{-}KI/LacZ\text{-}KI}$ × *Math5*$^{LacZ\text{-}KI/+}$	E12.5	E13.5	E14.5
Math5$^{LacZ\text{-}KI/+}$	181.7±3.8	413.3±11.1	658.7±26.9
Math5$^{LacZ\text{-}KI/LacZ\text{-}KI}$	2.3±0.4	7.7±1.1	NA
Math5$^{Math3\text{-}KI/LacZ\text{-}KI}$	3.32.3±0.4	40±1.33	87±7.33

Embryos from the same litter were used for comparison.
NA, not available.

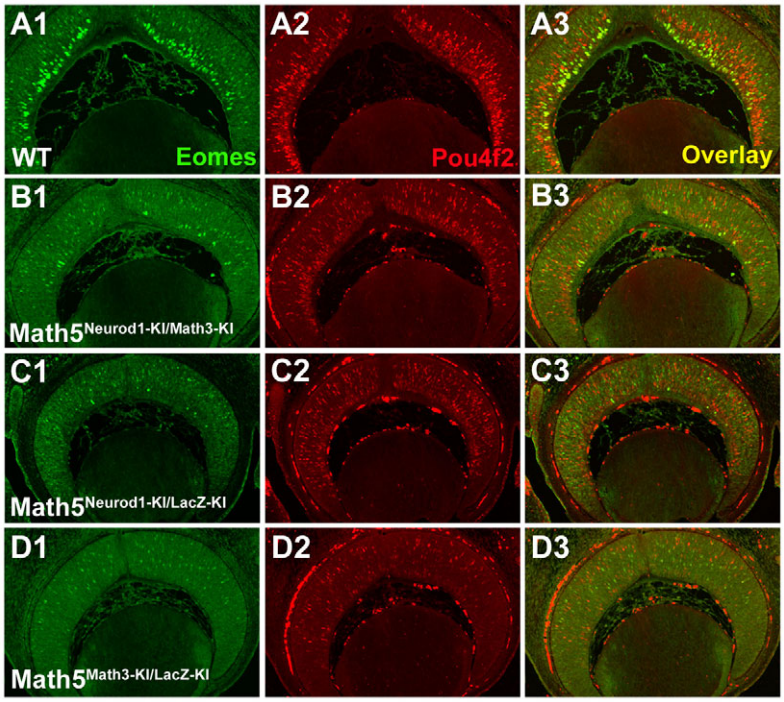

Fig. 5. Neurod1 is more effective than Math3 in activating *Eomes* in the absence of Math5. (**A1-D3**) Retinas from E14.5 embryos were immunostained with anti-Eomes (A1-D1) or anti-Pou4f2/Brn3b (A2-D2) antibodies. Merged images are shown in A3-D3. (A1-A3) Wild type, (B1-B3) *Math5*$^{Neurod1\text{-}KI/Math3\text{-}KI}$, (C1-C3) *Math5*$^{Neurodi\text{-}KI/lacZ\text{-}KI}$ and (D1-D3) *Math5*$^{Math3\text{-}KI/lacZ\text{-}KI}$.

DISCUSSION

Our results demonstrate that Neurod1, and to a lesser extent Math3, can replace Math5 to direct RPCs towards an RGC fate. Expressing *Neurod1* at the *Math5* locus in the absence of Math5 resulted in a substantial restoration of all aspects of RGC differentiation, including axonogenesis and formation of the optic nerve. Neurod1 was better at replacing Math5 than was Math3, but the presence of both factors appeared to have an optimal effect. One possible explanation for this is that Neurod1 and Math3 may have somewhat different DNA-binding propensities and thus activate distinct sets of Math5 target genes. In the retinas of *Neurod1* knock-in embryos, fewer cells expressed genes that mark the onset of RGC differentiation; only 30-40% of the number of wild-type RGCs was optimally observed in the knock-in retinas. Although we did not perform a quantitative analysis of RGC gene expression, both in situ hybridization and immunostaining analyses indicated that on a per cell basis, gene expression levels between knock-in and wild-type embryos were comparable. This suggests that a threshold level of Neurod1 protein is required to replace Math5 and that only a minority of RPCs expressing the knock-in alleles achieve this threshold. Accordingly, it might be expected that *Math5*$^{Neurod1\text{-}KI/Neurod1\text{-}KI}$ would have a stronger restorative effect than *Math5*$^{Neurod1\text{-}KI/lacZ\text{-}KI}$. However, we did not observe significant differences between these two genotypes (data not shown). In fact, *Math5*$^{Neurod1\text{-}KI/Math3\text{-}KI}$ resulted in slightly better effects, suggesting that one copy of *Neurod1* was sufficient to produce optimal restoration. These data imply that the threshold level of Neurod1 is modulated by other activity-limiting intrinsic factors, and one copy of *Neurod1* exhausts such factors.

Our study suggests that Neurod1 can be inserted into the RPC program to re-establish RGC competence and assume the roles that normally require Math5. However, the lack of over-production of amacrine cells in *Math5*$^{Neurod1\text{-}KI/Math3\text{-}KI}$ retinas suggests that, in addition to the ubiquitously expressed homeobox genes Pax6 and Six3, other factors are required to act with *Neurod1* and *Math3* to reprogram an RPC towards amacrine cell production. Precocious formation of amacrine cells may have occurred in *Math5*$^{Neurod1\text{–}KI/Math3\text{-}KI}$ retinas but may not have been tolerated in this slightly earlier environment. In fact, we have detected significant cell death within the central region of *Math5*$^{Neurod1\text{-}KI/Math3\text{-}KI}$ retinas as early as E11.5, whereas no increase in cell death was seen in E11.5 *Math5*-null retina (Le et al., 2006), suggesting improper and precocious cell differentiation may have taken place. The modest increase in the number of cone cells in *Math5*$^{Neurod1\text{-}KI/Math3\text{-}KI}$ retina indicates that a few *Math5*$^{Neurod1\text{-}KI/Math3\text{-}KI}$-expressing cells assume a cone cell fate – the next cell type to appear within the *Math5*-expressing cell lineage (Cayoutte et al., 2006). The results presented here support the view that an intrinsic program within the RPC dictates the functions of Neurod1 and Math3, when they are expressed at the *Math5* locus. Therefore, the specialized functions that have presumably evolved for these bHLH factors may not be as crucial in determining early retinal cell fates as is currently thought.

The intrinsic program necessary for a naïve RPC to advance to a specific competence state is thought to arise from a dynamic local external environment. This environment changes through time and continually provides instructions to RPCs to assume successive competence states (Cayouette et al., 2006; Wallace, 2008). The discovery of numerous transcriptional regulators essential for retinal cell fate specification and differentiation has lead to the elucidation of detailed genetic regulatory pathways that define the intrinsic programs of most RPCs (reviewed by Ohsawa and Kageyama, 2008; Mu and Klein, 2008). However, the mechanisms connecting the dynamic local environment within the developing retina to the intrinsic genetic programs that operate in distinct RPCs remain elusive.

Although we have emphasized the evidence that *Neurod1* is more capable of adapting to a foreign environment than *Math3*, our results also show that neither Neurod1 nor Math3 can fully restore RGCs in the absence of Math5. Neurod1 and Math3 together were slightly more effective that Neurod1 alone, which in turn was more effective than Math3 alone. Recently, it has been shown that a *Math5*$^{Mash1\text{-}KI}$

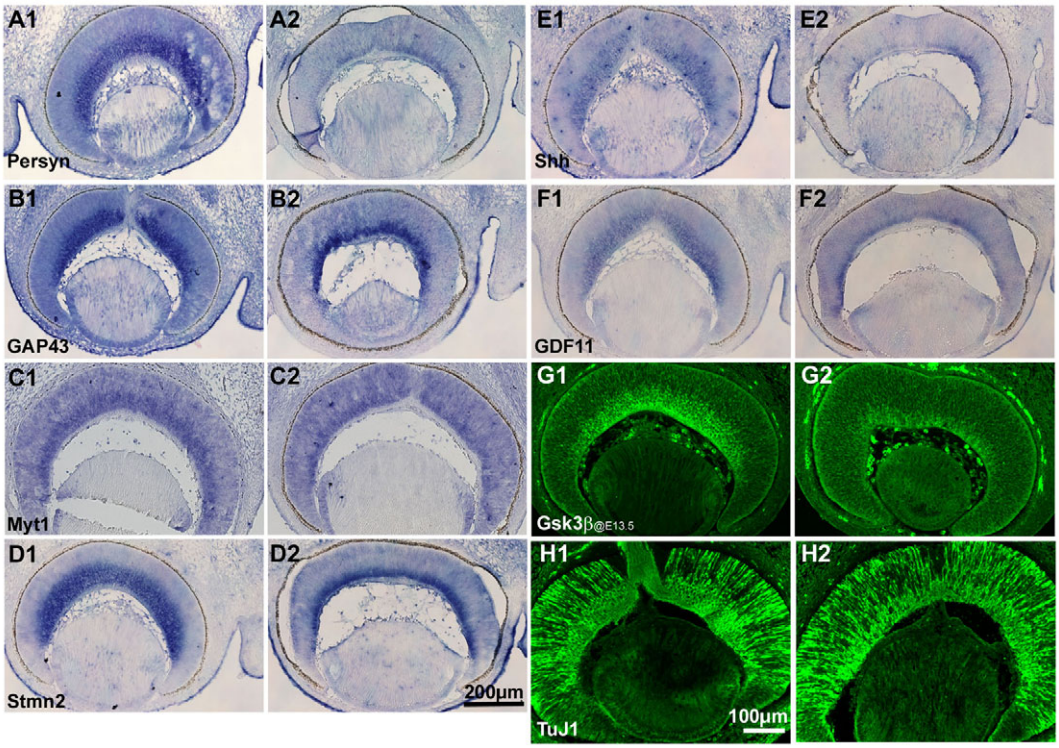

Fig. 6. Neurod1 and Math3 activate the RGC gene regulatory network in the absence of Math5. *Math5*$^{Neurod1\text{-}KI/Math3\text{-}KI}$ retinas from E14.5 (or E13.5 for G1,G2) embryos were analyzed by in situ hybridization (purple) or immunostaining (green). (**A1-H1**) Wild-type retinas. (**A2-H2**) *Math5*$^{Neurod1\text{-}KI/Math3\text{-}KI}$ retinas. In situ hybridization probes and antibodies for immunostaining representing genes downstream of Math5 are indicated in the lower left-hand corner in A1-H1.

allele has only modest restorative ability (Nadean Brown, personal communication). The obvious explanation for these differences is that all of these bHLH factors have amino acid sequence differences within and outside of their bHLH domains that are likely to reflect differences in protein-protein interactions, post-translational modifications, and promoter-enhancer preferences. For example, three amino acids within the basic domain of chicken Ath5 are reported to be crucial for protein-protein interactions that confer DNA binding specificity to Ath5 (Skowronska-Krawczyk et al., 2005). These residues are found in Math5 but not in Neurod1, Math3 or Mash1 (see Table S3 in the supplementary material). The helix 1 and helix 2 domains within Mash1 and Math1 are crucial in determining neuronal differentiation (Nakada et al., 2004). Thus, the sequence differences in helix 1 and helix 2 domains among Math5, Neurod1, Math3 or Mash1 might account for their differential function in the same environment (see Table S3 in the supplementary material).

In their normal cellular context, Math5, Neurod1 and Math3 are likely to regulate the expression of distinct sets of target genes during retinal development. Recent reports have identified downstream target genes for Math5, but there is little information on the overlap of these target genes with the genes regulated by Neurod1 and Math3 (Mu et al., 2005; Del Bene et al., 2007). Moreover, differences in cellular context could result in post-translational modifications that affect DNA-binding site choice. In *Xenopus*, a post-translational mechanism mediated by GSK-3β phosphorylation negatively regulates the ability of NeuroD to promote RGC differentiation (Moore et al., 2002). Although mouse Neurod1 lacks the GSK-3β phosphorylation site, other kinases such as ERK may modulate the function of Neurod1 when it is expressed at the *Math5* locus in *Math5*-expressing RPCs (Dufton et al., 2005).

Several studies have reported on the effects of replacing one related transcription factor with another in a developmental context. In many cases, gene swapping demonstrates a large degree of functional redundancy and indicates that the timing of expression is perhaps more crucial than specialized functions that might have evolved. For example, in the retina, the closely related POU domain factors Pou4f1 and Pou4f2 appear to be interchangeable in their ability to function as regulators of RGC differentiation if they are expressed at the *Pou4f2* locus (Pan et al., 2005). In mid-hindbrain development, the lethal En1 mutant phenotype can be rescued by replacing En1 with closely related En2 (Hanks et al., 1995). However, two related bHLH genes, *Mash1* and *Ngn2*, have been shown to maintain their divergent functions in the specification of neuronal subtype identity in the dorsal telencephalon and ventral spinal cord (Parras et al., 2002). In skeletal muscle, the myogenic bHLH regulatory factor myogenin can substitute for the closely related Myf5 factor in promoting myogenesis, although less efficiently (Wang and Jaenisch, 1997). The same swap leads to complete rescue of the lethal Myf5 mutant rib phenotype (Wang et al., 1996). Similarly, in the sensory nervous system of *Drosophila*, the proneural bHLH factor Amos, a bHLH factor closely related to Atonal, can substitute for Atonal in specifying R8 photoreceptor fate (Maung and Jarman, 2007), whereas another bHLH factor, Sc, cannot (Sun et al., 2000). By contrast, Amos cannot rescue the chordotonal phenotype seen in *Atonal* mutants (Maung and Jarman, 2007), suggesting that the developmental context is critical for

distinct bHLH factors to exert their specific activity. Our current study suggests that developmental time and the intrinsic properties within distinct RPCs largely dictate the roles of bHLH factors in specifying early retinal cell fate.

In the developing retina, bHLH factors and other transcriptional regulators produce a highly complex combinatorial state that defines each RPC subpopulation (Ohsawa and Kageyama, 2008; Mu and Klein, 2008; Mu et al., 2008). Thus, each subpopulation is under the control of a specific gene regulatory network composed of hierarchical tiers of transcription factors connected to their *cis* regulatory sites on target regulatory genes (Ben-Tabou de-Leon and Davidson, 2007). Although each network is distinct, its underlying framework is likely to be similar to that of other RPC subpopulation. The crucial nodes in the different RPC networks are likely to be represented by transcription factors of the same class. There is little question that bHLH factors have evolved specialized features for each lineage, but the fact that they are sometimes interchangeable reflects the flexibility of RPC gene regulatory networks. A given network can tolerate the replacement of one bHLH factor with another, provided the other factor has the capability of fitting into the network at the correct hierarchical level to receive the inputs and transmit the outputs that are required for successful network operation.

We thank Jan Parker-Thornburg, Sandra Rivera and the Genetically Engineered Mouse Facility at The University of Texas M. D. Anderson Cancer Center for generating the knock-in mouse lines. We also acknowledge the assistant of Jodie Polan for confocal microscopy and imaging, and Eric Meadows for qRT-PCR analysis. We thank Satchidananda Panda for providing the anti-melanopsin antibody and acknowledge the M. D. Anderson Cancer Center DNA Analysis Facility for DNA sequencing. We are grateful for insightful comments on the manuscript provided by Xiuqian Mu. The Genetically Engineered Mouse Facility and DNA Analysis Facility are supported in part by a National Cancer Institute Cancer Center Core Grant (CA016672). The work was supported by grants to W.H.K. from the National Eye Institute (EY011930 and EY010608-139005) and from the Robert A. Welch Foundation (G-0010), and by a grant from the E. Matilda Ziegler Foundation for the Blind to S.W.W.

Supplementary material

Supplementary material for this article is available at
http://dev.biologists.org/cgi/content/full/135/20/3379/DC1

References

Akagi, T., Inoue, T., Miyoshi, G., Bessho, Y., Takahashi, M., Lee, J. E., Guillemot, F. and Kageyama, R. (2004). Requirement of multiple basic helix-loop-helix genes for retinal neuronal subtype specification. *J. Biol. Chem.* **279**, 28492-28498.

Bäumer, N., Marquardt, T., Stoykova, A., Spieler, D., Treichel, D., Ashery-Padan, R. and Gruss, P. (2003). Retinal pigmented epithelium determination requires the redundant activities of Pax2 and Pax6. *Development* **130**, 2903-2915.

Ben-Tabou de-Leon, S. and Davidson, E. H. (2007). Gene regulation: gene control network in development. *Annu. Rev. Biophys. Biomol. Struct.* **36**, 191-212.

Brown, N. L., Kanekar, S., Vetter, M. L., Gemza, D. L. and Glaser, T. (1998). Math5 encodes a basic helix-loop-helix transcription factor expressed during early stages of retinal neurogenesis. *Development* **125**, 4821-4833.

Brown, N. L., Patel, S., Brzezinski, J. and Glaser, T. (2001). Math5 is required for retinal ganglion cell and optic nerve formation. *Development* **128**, 2497-2508.

Cayouette, M., Poggi, L. and Harris, W. A. (2006). Lineage in the vertebrate retina. *Trends Neurosci.* **29**, 563-570.

Coombs, J., van der List, D., Wang, G. Y. and Chalupa, L. M. (2006). Morphological properties of mouse retinal ganglion cells. *Neuroscience* **140**, 123-136.

Del Bene, F., Ettwiller, L., Skowronska-Krawczyk, D., Baier, H., Matter, J. M., Birney, E. and Wittbrodt, J. (2007). In vivo validation of a computationally predicted conserved Ath5 target gene set. *PLoS Genet.* **3**, 1661-1671.

Dufton, C., Marcora, E., Chae, J. H., McCullough, J., Eby, J., Hausburg, M., Stein, G. H., Khoo, S., Cobb, M. H. and Lee, J. E. (2005). Context-dependent regulation of NeuroD activity and protein accumulation. *Mol. Cell. Neurosci.* **28**, 727-736.

Elshatory, Y., Deng, M., Xie, X. and Gan, L. (2007). Expression of the LIM-homeodomain protein Isl1 in the developing and mature mouse retina. *J. Comp. Neurol.* **503**, 182-197.

Gan, L., Wang, S. W., Huang, Z. and Klein, W. H. (1999). POU domain factor Brn-3b is essential for retinal ganglion cell differentiation and survival but not for initial cell fate specification. *Dev. Biol.* **210**, 469-480.

George, S. H., Gertsenstein, M., Vintersten, K., Korets-Smith, E., Murphy, J., Stevens, M. E., Haigh, J. J. and Nagy, A. (2007). Developmental and adult phenotyping directly from mutant embryonic stem cells. *Proc. Natl. Acad. Sci. USA* **104**, 4455-4460.

Hanks, M., Wurst, W., Anson-Cartwright, L., Auerbach, A. B. and Joyner, A. L. (1995). Rescue of the En-1 mutant phenotype by replacement of En-1 with En-2. *Science* **269**, 679-682.

Hatakeyama, J. and Kageyama, R. (2004). Retinal cell fate determination and bHLH factors. *Semin. Cell. Dev. Biol.* **15**, 83-89.

Inoue, T., Hojo, M., Bessho, Y., Tano, Y., Lee, J. E. and Kageyama, R. (2002). Math3 and NeuroD regulate amacrine cell fate specification in the retina. *Development* **129**, 831-842.

Kim, J., Lander, A. L., Lyons, K. M., Matzuk, M. M. and Calof, A. L. (2005). GDF11 controls the timing of progenitor cell competence in developing retina. *Science* **308**, 1927-1930.

Lagutin, O., Zhu, C., Furuta, Y., Rowitch, D., McMahon, A. P. and Oliver, G. (2001). Six3 promotes the formation of ectopic optic vesicle-like structures in mouse embryos. *Dev. Dyn.* **221**, 342-349.

Le, T. T., Wroblewski, E., Patel, S., Riesenberg, A. N. and Brown, N. L. (2006). Math5 is required for both early retinal neuron differentiation and cell cycle progression. *Dev. Biol.* **295**, 764-778.

Ledent, V., Paquet, Q. and Vervoort, M. (2002). Phylogenetic analysis of the human basic helix-loop-helix proteins. *Genome Biol.* **3**, RESEARCH0030.

Lin, B., Wang, S. W. and Masland, R. H. (2004). Retinal ganglion cell type, size, and spacing can be specified independent of homotypic dendritic contacts. *Neuron* **43**, 475-485.

Livesey, F. J. and Cepko, C. L. (2001). Vertebrate neural cell-fate determination: lessons from the retina. *Nat. Rev. Neurosci.* **2**, 109-118.

Mao, C. A., Kiyama, T., Pan, P., Furuta, Y., Hadjantonakis, A. K. and Klein, W. H. (2008). Eomesodermin, a target gene of Pou4f2, is required for retinal ganglion cell and optic nerve development in the mouse. *Development* **135**, 271-280.

Maung, S. M. and Jarman, A. P. (2007). Functional distinctness of closely related transcription factors: a comparison of the Atonal and Amos proneural factors. *Mech. Dev.* **124**, 647-656.

Moore, K. B., Schneider, M. L. and Vetter, M. L. (2002). Postranslational mechanisms control the timing of bHLH function and regulate retinal cell fate. *Neuron* **34**, 183-195.

Moshiri, A., Gonzalez, E., Tagawa, K., Maeda, H., Wang, M., Frishman, L. J. and Wang, S. W. (2008). Near complete loss of retinal ganglion cells in the *math5/brn3b* double knockout elicits severe reductions of other cell types during retinal development. *Dev. Biol.* **316**, 214-227.

Mu, X. and Klein, W. H. (2004). A gene regulatory hierarchy for retinal ganglion cell specification and differentiation. *Semin. Cell Dev. Biol.* **15**, 15-23.

Mu, X. and Klein, W. H. (2008). Gene regulatory networks and the development of retinal ganglion cells. In *Eye, Retina, and Visual System of the Mouse* (ed. L. M. Chalupa and R. W. Williams), pp. 321-332. Cambridge, MA: MIT Press.

Mu, X., Beremand, P. D., Zhao, S., Pershad, R., Sun, H., Scarpa, A., Liang, S., Thomas, T. L. and Klein, W. H. (2004). Discrete gene sets depend on POU domain transcription factor Brn3b/Brn-3.2/POU4f2 for their expression in the mouse embryonic retina. *Development* **131**, 1197-1210.

Mu, X., Fu, X., Sun, H., Beremand, P. D., Thomas, T. L. and Klein, W. H. (2005). A gene network downstream of transcription factor Math5 regulates retinal progenitor cell competence and ganglion cell fate. *Dev. Biol.* **280**, 467-481.

Mu, X., Fu, X., Beremand, P. D., Thomas, T. L. and Klein, W. H. (2008). Gene regulatory logic in retinal ganglion cell development: Isl1 defines a critical branch distinct from but overlapping with Pou4f2. *Proc. Natl. Acad. Sci. USA* **105**, 6942-6947.

Nakada, Y., Hunsaker, T. L., Henke, R. M. and Johnson, J. E. (2004). Distinct domains within Mash1 and Math1 are required for function in neuronal differentiation versus neuronal cell-type specification. *Development* **131**, 1319-1330.

Ohsawa, R. and Kageyama, R. (2008). Regulation of retinal cell fate specification by multiple transcription factors. *Brain Res.* **1192**, 90-98.

Pan, L., Yang, Z., Feng, L. and Gan, L. (2005). Functional equivalence of Brn3 POU-domain transcription factors in mouse retinal neurogenesis. *Development* **132**, 703-712.

Pan, L., Deng, M., Xie, X. and Gan, L. (2008). ISL1 and BRN3B co-regulate the differentiation of murine retinal ganglion cells. *Development* **135**, 1981-1990.

Parras, C. M., Schuurmans, C., Scardigli, R., Kim, J., Anderson, D. J. and Guillemot, F. (2002). Divergent functions of the proneural genes Mash1 and Ngn2 in the specification of neuronal subtype identity. *Genes Dev.* **16**, 324-338.

Rachel, R. A., Dolen, G., Hayes, N. L., Lu, A., Erskine, L., Nowakowski, R. S. and Mason, C. A. (2002). Spatiotemporal features of early neurogenesis differ in wild-type and albino mouse retina. *J. Neurosci.* **22**, 4249-4263.

Skowronska-Krawczyk, D., Matter-Sadzinski, L., Ballivet, M. and Matter, J. M. (2005). The basic domain of ATH5 mediates neuron-specific promoter activity during retina development. *Mol. Cell. Biol.* **25**, 10029-10039.

Sun, W., Li, N. and He, S. G. (2002). Large-scale morphological survey of mouse retinal ganglion cells. *J. Comp. Neurol.* **451**, 115-126.
Sun, Y., Jan, L. Y. and Jan, Y. N. (2000). Ectopic scute induces Drosophila ommatidia development without R8 founder photoreceptors, *Proc. Natl. Acad. Sci. USA* **97**, 6815-6819.
Tokuoka, H., Yoshida, T., Matsuda, N. and Mishina, M. (2002). Regulation by glycogen synthase kinase-3beta of the arborization field and maturation of retinotectal projection in zebrafish. *J. Neurosci.* **22**, 10324-10332.
Tomita, K., Moriyoshi, K., Nakanishi, S., Guillemot, F. and Kageyama, R. (2000). Mammalian achaete-scute and atonal homologs regulate neuronal versus glial fate determination in the central nervous system. *EMBO J.* **19**, 5460-5472.
Trimarchi, J. M., Stadler, M. B. and Cepko, C. L. (2008). Individual retinal progenitor cells display extensive heterogeneity of gene expression. *PLoS ONE* **3**, e1588.
Vetter, M. L. and Brown, N. L. (2001). The role of basic helix-loop-helix genes in vertebrate retinogenesis. *Semin. Cell Dev. Biol.* **12**, 491-498.
Wallace, V. A. (2008). Proliferative and cell fate effects of Hedgehog signaling in the vertebrate retina. *Brain Res.* **1192**, 61-75.
Wang, J. C. and Harris, W. A. (2005). The role of combinational coding by homeodomain and bHLH transcription factors in retinal cell fate specification. *Dev. Biol.* **285**, 101-115.
Wang, S. W., Kim, B. S., Ding, K., Wang, H., Sun, D., Johnson, R. L., Klein, W. H. and Gan, L. (2001). Requirement for math5 in the development of retinal ganglion cells. *Genes Dev.* **15**, 24-29.
Wang, Y. and Jaenisch, R. (1997). Myogenin can substitute for Myf5 in promoting myogenesis but less efficiently. *Development* **124**, 2507-2513.
Wang, Y., Schnegelsberg, P. N., Dausman, J. and Jaenisch, R. (1996). Functional redundancy of the muscle-specific transcription factors Myf5 and myogenin. *Nature* **379**, 823-825.
Yang, Z., Ding, K., Pan, L., Deng, M. and Gan, L. (2003). Math5 determines the competence state of retinal ganglion cell progenitors. *Dev. Biol.* **264**, 240-254.